

A study of the Jovian "energetic magnetospheric events" observed by Galileo: role in the radial plasma transport

Philippe Louarn

Centre d'Etudes Spatiales des Rayonnements - CNRS, Toulouse, France

Alain Roux, Sylvaine Perraut

Centre d'etude des Environnements Terrestre et Planetaires - CNRS, Velizy, France

William S. Kurth and Donald A. Gurnett

University of Iowa, Iowa City

Abstract. Using the Galileo Plasma Wave Subsystem (PWS) experiment, we analyze the large-scale energetic events that recurrently occur in the Jovian magnetosphere. As described by Louarn *et al.* [1998], these sporadic phenomena are associated with enhancements in the flux of the various auroral radio emissions, with the creation of new sources of radiation in the Io torus, and correspond to large fluctuations in the magnetodisc density. These events have been interpreted as sudden releases of energy in the Jovian magnetosphere. In order to better characterize them we study an extended PWS data set (orbits G2, G7, and G8) corresponding to 130 days of observations during which 32 energetic events have been unambiguously identified. We conclude the following: (1) The periods of enhanced energy releases in the magnetosphere (as indicated by increases in the auroral radio flux) are almost systematically initiated by an energetic event. (2) The periodicity of the events changes from one orbit to the other and it is shown that the more frequent they are, the denser is the plasma sheet. (3) In a large majority of cases the events occur as the disc is thin and relatively depleted in plasma. A few hours after the events, a thick and heavily populated magnetodisc is observed. It then thins, and its density progressively decreases over a timescale of a few tens of hours. Our interpretation is that the events correspond to sequences of rapid plasma loading of the magnetodisc that are followed by much more progressive evacuations of the magnetodisc plasma. The global plasma content of the magnetodisc would thus increase with their frequency. This study suggests that the energetic events are related to an instability developing in the external part of the Io torus or in the close magnetodisc that sporadically injects new plasma populations in the more distant magnetodisc. The associated transport process appears to be efficient enough to explain the outward evacuation of a significant fraction of the plasma created at the Io orbit (a few 10^{28} ions/s).

1. Introduction

The existence of a large-scale bursty activity of the Jovian magnetosphere was reported recently [Louarn *et al.*, 1998 hereafter referred to as L98; Krupp *et al.*, 1998; Woch *et al.*, 1998]. As seen from the Galileo Plasma Wave Subsystem (PWS), this activity can be described as the quasiperiodic occurrence of "events" corresponding to global increases in the flux of various Jovian radio emissions and to spectro/temporal modifications of their morphology. These energetic events are characterized by the simultaneous observation of (1) enhanced auroral radio emissions, (2) creation of new sources of narrowband kilometric radiation (n-KOM), and (3) fluctuations in the cutoff frequency of the continuum radiation. They typically last a few hours and have shown a periodicity of the order of 70 hours during the September/October 1996 period analyzed in L98.

Even if the generation mechanisms of these different emissions are still not completely understood, their origin is sufficiently documented to allow for a qualitative interpretation of the observations. As a matter of fact, (1) it is widely admitted that the flux of the auroral radio emissions is linked to the flux of the accelerated auroral electrons (see the review by Zarka [1998]), (2) the sources of the n-KOM emissions are localized in the outermost regions of the Io torus [Kaiser and Desch, 1980; Jones, 1987; Leblanc, 1987; Reiner *et al.*, 1993] and, (3) the cutoff of the continuum radiation gives an estimate of the local plasma frequency [Gurnett *et al.*, 1980; Perraut *et al.*, 1998]. The energetic events are therefore large-scale phenomena characterized by (1) an increase in the auroral precipitation, (2) the simultaneous development of activity in the Io torus at a typical Jovian distance of 10 R_j (Jovian radii), and (3) changes in the plasma density or in the thickness of the plasma sheet (seen at distances larger than 30 R_j). Other Galileo instruments, the high-energy particle detectors and the magnetometer, show that the energetic events are also associated with radial flows of energetic particles and with magnetic perturbations in the current sheet [Krupp *et al.*,

Copyright 2000 by the American Geophysical Union.

Paper number 1999JA900478
0148-0227/00/1999JA900478\$09.00

1998; *Woch et al.*, 1998]. Since the flux of the auroral radio emissions is likely linked to the magnetospheric energy dissipation rate (see *Kurth and Gurnett* [1998] for a discussion in the terrestrial case), the energetic events likely correspond to sudden energy releases in the Jovian magnetosphere. They thus present some analogies with terrestrial substorms, and it is tempting to interpret them as an important type of magnetospheric activity.

The discovery of this bursty activity renews the ideas concerning the Jovian magnetospheric dynamics. In contrast with the terrestrial situation, Jupiter is indeed remarkable by its permanent and powerful auroral UV, optical, and radio emissions. They constitute evidence for the existence of a continuous energy release in the magnetosphere; a situation sometimes compared to binary systems (the Jupiter/Io couple) and/or to pulsars (magnetosphere in fast rotation) [*Goldreich and Lynden-Bell*, 1969; *Kennel and Coroniti*, 1975; *Dessler*, 1983; *Hill et al.*, 1983; *Vasyliunas*, 1983]. In the inner magnetosphere ($L < 6$) the permanent activity (or the permanent energy release) is linked to the motion of Io which gives rise to specific decametric radio emissions (the "Io-related" decametric radiation) and to auroral UV emissions [see *Prangé et al.*, 1996]. On higher L shells, in association with a stable auroral arc (see, for example, *Gérard et al.* [1993] and auroral images published later) and to a permanent generation of radio emissions from the decametric to the kilometric range [*Ladreitner et al.*, 1994], another type of magnetospheric activity exists. Its origin is still not clearly understood. It could be related to departures from the ideal MHD (existence of a finite parallel potential drop) in the ionosphere/magnetosphere current system that enforces the plasma corotation (see, for example, *Hill*, [1979]; *Hill et al.*, [1983] for studies related with this current system) and/or, farther from the planet, to a regular loss of the centrifugal energy of the magnetodisc due to a still not identified mechanism. Whatever the details, it is now widely admitted that the planetary rotation is the dominant source of energy for this permanent magnetospheric activity (unlike the case of the Earth where the activity is driven by the solar wind). The energetic events appear to be superimposed on this permanent activity. One can interpret them in two radically different ways. They can be (1) "substorm-like", thus corresponding to releases of the magnetic energy accumulated in the magnetosphere under the control of the solar wind or (2) explosive dissipations of the centrifugal energy accumulated in the inner magnetosphere, because of the permanent plasma loading at the Io orbit. More complex situations can also be imagined. For example, a role of the solar wind at triggering phases of enhanced dissipation of the centrifugal energy is possible. This would explain the observations of solar wind effects in the Jovian magnetospheric activity (see, for example, *Zarka and Genova* [1983], *Desch and Barrow* [1984], *Barrow and Desch* [1989], and *Kaiser* [1993]). Even if the events could be fundamentally different from terrestrial substorms (dissipation of centrifugal energy rather than magnetic energy), an influence of the solar wind in their triggering is then not excluded.

In the present article, we try to describe the nature of the energetic events by using the radio emissions as a diagnostic tool of the magnetospheric activity. In particular, we will show that the energetic events are associated to important

variations of the magnetodisc/plasma sheet density and that they likely correspond to significant redistributions of the plasma from the Io torus to the outer magnetosphere. In that sense, our study is connected to the general problem of the radial plasma transport across the magnetosphere (see, for example, *Hill and Dessler* [1991], *Ferrière and Blanc* [1996], *Ferrière et al.* [1999] for general presentations and, for some more specific discussions: *Hill* [1976], *Southwood and Kivelson* [1987], *Pontius and Hill* [1989], *Fazakerley and Southwood* [1992], *Yang et al.* [1994], *Kivelson et al.* [1997], and additional references therein). As developed in the present study, we propose a global sketch in which the sporadic activity of the Jovian magnetosphere and the radial plasma transport are closely related, the main point being that the energetic events are associated with sudden plasma loading of the magnetodisc.

Our analysis is based on data recorded during the orbits G2, G7, and G8 over a 9-month period. This large data set, presented in section 2, is used for a statistical analysis of the activity and for a discussion of its long-term evolution (section 3). Its relationship with the variations of the density in the magnetodisc is studied in section 4. Quantitative estimates of the efficiency of the plasma transport phenomena are performed in section 5 before the conclusions (section 6) where a scenario of a radial plasma transport, related to the occurrence of the energetic events, is proposed.

2. Presentation of the PWS Observations

In Plates 1, 2 and 3, PWS observations recorded during orbit G2 (51 days of data, from DOY 96-245 to 96-295), orbit G7 (34 days of data, from DOY 97-078 to 97-111), and orbit G8 (45 days of data, from DOY 97-125 to 97-169) are presented using the same temporal scale. The original data consist of electric and magnetic spectra, recorded alternately every 18.7 s and measured from 5.6 Hz to 5.6 MHz for the electric field (see *Gurnett et al.* [1992] for a description of the PWS experiment).

In Plates 1a - 1c, 2a - 2c, and 3a - 3c, parts of the original electric spectra, coded from black to red as the wave intensity increases (classical "rainbow" color code), are shown in a very compressed form. They correspond to frequency domains of radio emissions having a particular magnetospheric origin (see *Kurth et al.* [1998] for a review of the Jovian radio emissions).

1. The high-frequency emission (above 300-500 kHz) seen in Plates 1a, 2a, and 3a (dynamic spectra above 50 kHz) is the hectometric (HOM) and the low-frequency part of the decametric radiation (DAM). They are generated in the auroral zones, at frequencies close to the electron gyrofrequency, probably by a microscopic instability driven by accelerated electrons: the cyclotron maser instability. At lower frequencies (around 100 - 200 kHz) a narrowband emission presenting a pronounced 10-hour periodicity is detected: the n-KOM. In the same frequency domain a bursty radiation, the b-KOM (for broadband kilometric radiation), is also sometimes observed. It is particularly apparent on G7 (for example, around DOY 97-095) and on G8 data. This radiation is simply a low-frequency extension of higher-frequency auroral radio emissions. In the rest of the paper, the distinction between b-KOM, HOM, and DAM will no longer

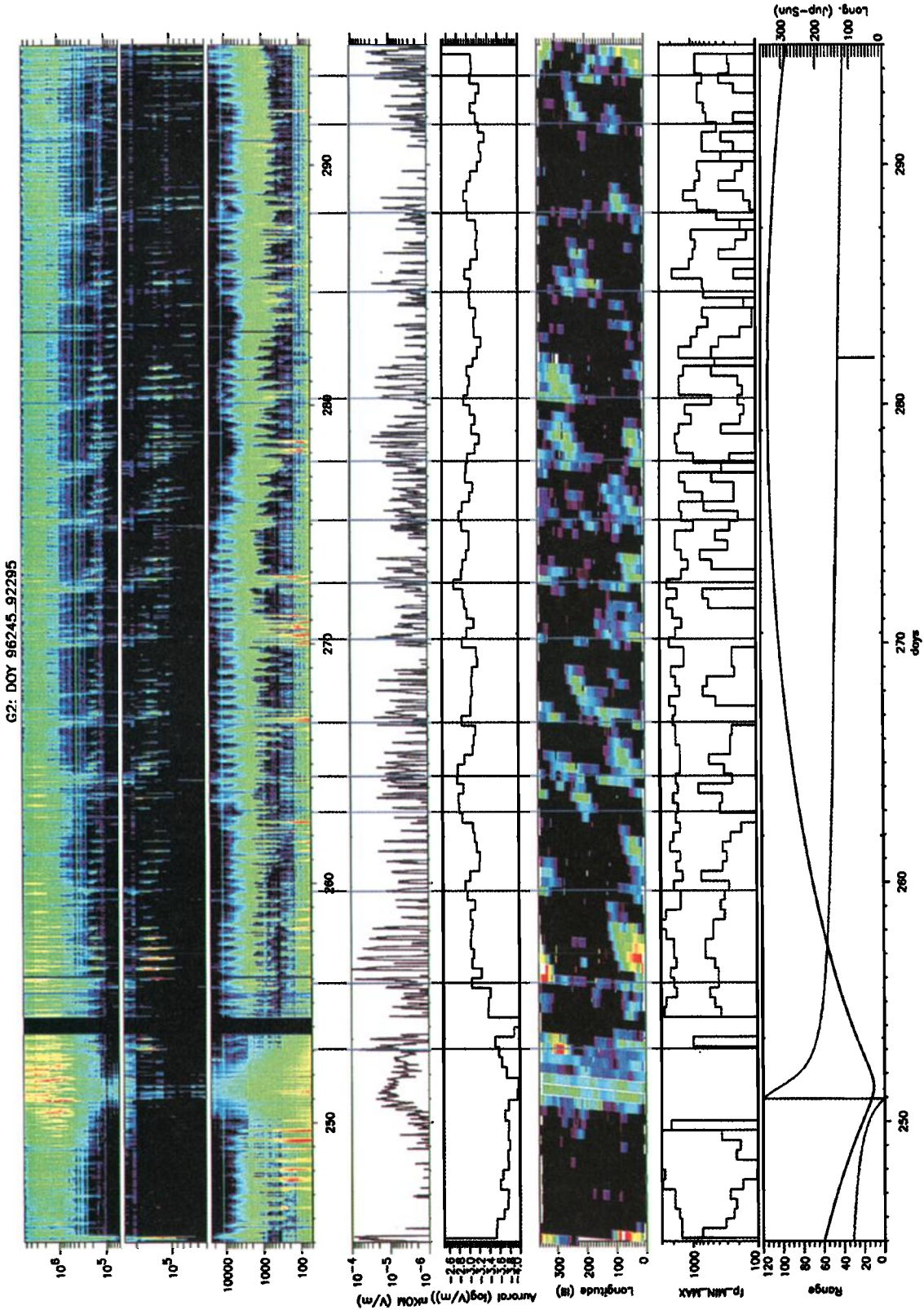


Plate 1. An overview of the Plasma Wave Subsystem (PWS) observations performed during the G2 orbit. From top to bottom: Dynamic spectra corresponding to (a) auroral emissions, (b) Io torus emissions (n-KOM) and, (c) continuum radiation. Averaged wave intensity (in V/m) for: (d) n-KOM, and (e) auroral emissions. (f): expected position (in system III longitude) of the n-KOM sources in the Io torus. (g): maximum and minimum plasma frequency measured at the crossings of the disc (for each planetary rotations). (h) position of Galileo: thin line, longitude with respect to the Jovian-Sun axis; thick line, radial distance.

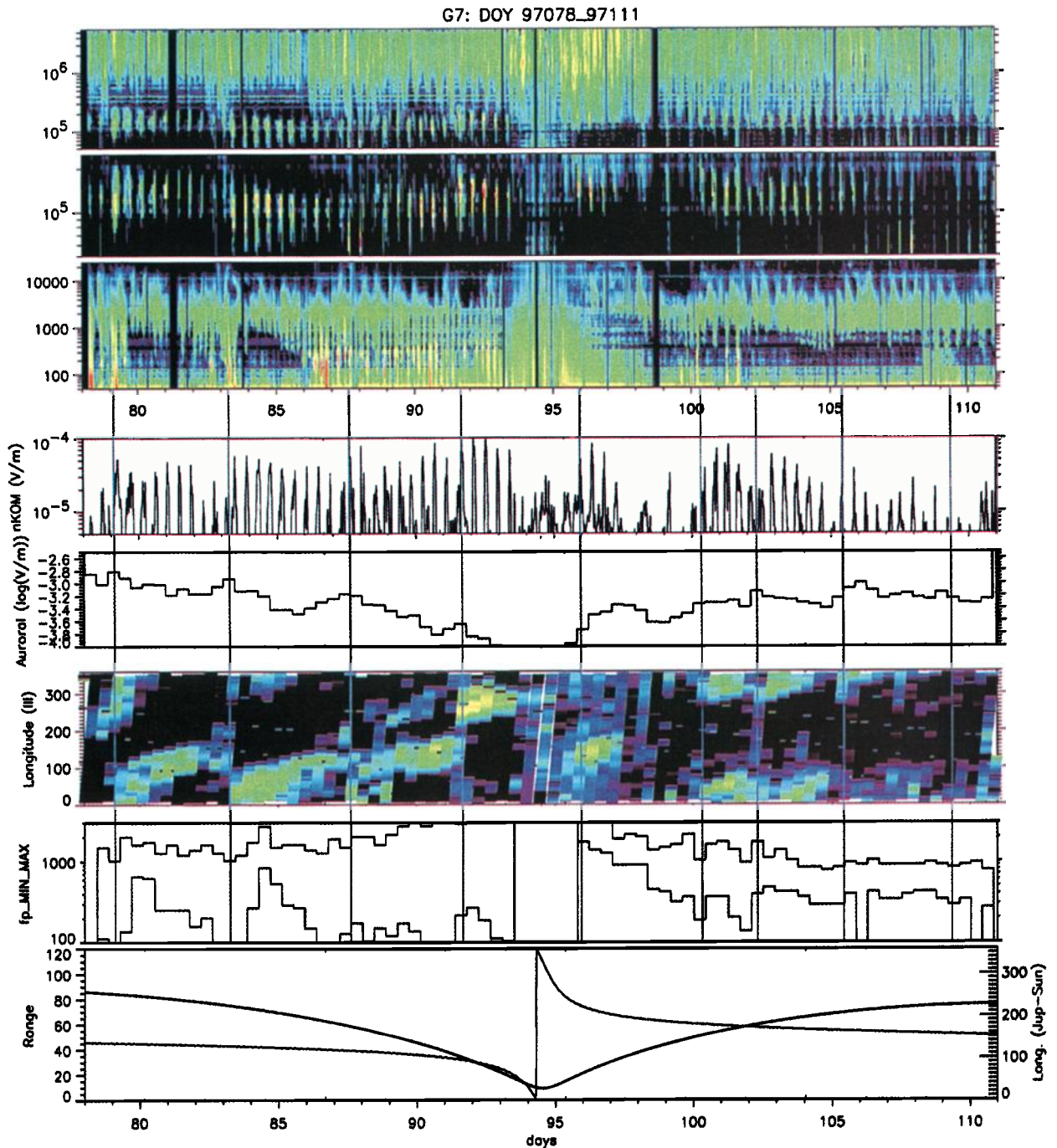


Plate 2. An overview of the Plasma Wave Subsystem (PWS) observations performed during the G7 orbit. From top to bottom: Dynamic spectra corresponding to (a) auroral emissions, (b) Io torus emissions (n-KOM) and, (c) continuum radiation. Averaged wave intensity (in V/m) for: (d) n-KOM and, (e) auroral emissions. (f): expected position (in system III longitude) of the n-KOM sources in the Io torus. (g): maximum and minimum plasma frequency measured at the crossings of the disc (for each planetary rotations). (h) position of Galileo: thin line, longitude with respect to the Jovian-Sun axis; thick line, radial distance.

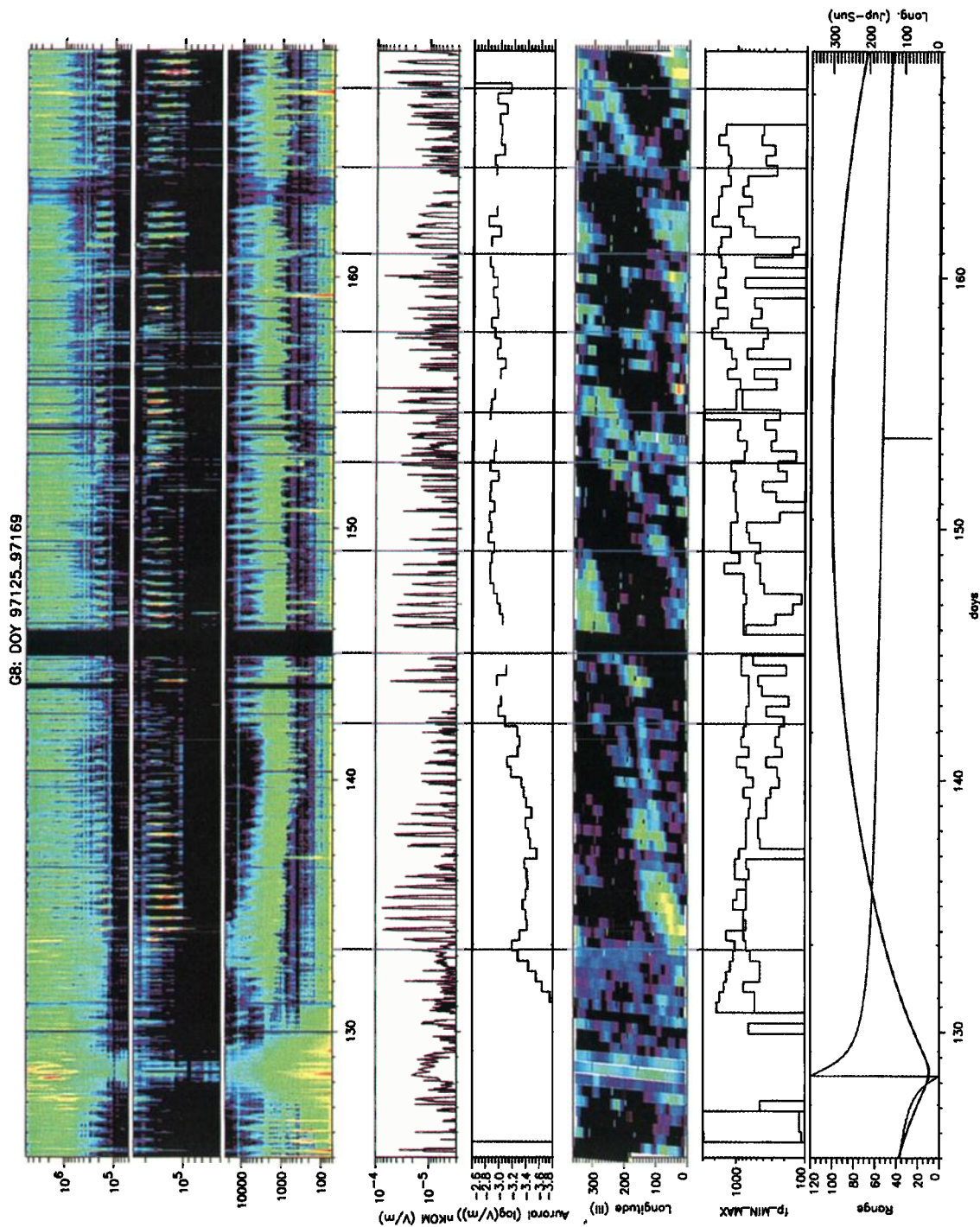


Plate 3. An overview of the Plasma Wave Subsystem (PWS) observations performed during the G8 orbit. From top to bottom: Dynamic spectra corresponding to (a) auroral emissions, (b) Io torus emissions (n-KOM) and, (c) continuum radiation. Averaged wave intensity (in V/m) for: (d) n-KOM and, (e) auroral emissions. (f): expected position (in system III longitude) of the n-KOM sources in the Io torus. (g): maximum and minimum plasma frequency measured at the crossings of the disc (for each planetary rotations). (h) position of Galileo: thin line, longitude with respect to the Jovian-Sun axis; thick line, radial distance.

be made. By reference to their common origin (magnetic field lines connected to high latitude regions, see *Ladreiter et al.* [1994]), we will call them "auroral radio emissions".

2. The n-KOM is specifically shown in Plates 1b, 2b, and 3b (dynamic spectra from 50 to 250 kHz). Its organization in regular flashes is explained by the rotation of its sources that are localized in the outermost regions of the Io torus [*Reiner et al.* 1993]. The b-KOM has been removed which helps to distinguish the variations in the n-KOM morphology. The recurrent creations of new sources (for example at DOY 96-264.5, 96-266.7) are well apparent. Once formed, the sources seem to progressively weaken and, over a variable period of time (from 2-3 Jovian rotations to more than 15), finally vanish (for example, at DOY 96-266, 96-269). It is believed that the n-KOM emission is generated via a mode conversion from electrostatic upper hybrid emissions, however, the details of its generation are still unknown. Nevertheless, we will interpret the creation of a new n-KOM source as an indication of the development of a particular activity in the outermost regions of the Io torus.

3. Plates 1c, 2c, and 3c (below 25 kHz) correspond to the frequency domain of the continuum radiation. This emission is detected almost everywhere in the magnetospheric cavity [*Kurth et al.*, 1979, 1998]. It presents a very clear low-frequency cut-off at, or very close to, the plasma frequency. This will be used for determining the local plasma density. Its 5-hour modulation is due to the wobbling of the magnetodisc and indicates that Galileo, located close to the equatorial plane, regularly crosses the plasma sheet.

Plates 1d, 2d, and 3d are time series of the integrated flux of the n-KOM. The spectral amplitude of the wave electric field measured by PWS (unit: $Vm^{-1}Hz^{-1/2}$) is here integrated from 70 to 160 kHz. Plates 1e, 2e, and 3e are similar to Plates 1d, 2d and 3d but concern the auroral emissions (integration from 1 to 5.6 MHz). As already mentioned, this quantity will be used for surveying the auroral activity. In order to remove short-scale fluctuations, the flux is here averaged over each Jovian rotation. The effect of the Galileo trajectory is

corrected by normalizing the flux to the distance of 50 R_j . One notes that rather surprisingly the corrected flux becomes small close to Jupiter (for $r < 30 R_j$, where r is the Galileo/Jupiter distance) which can be interpreted as an effect of the beaming of the auroral radio emissions. Plates 1f, 2f, and 3f is a particular presentation of the integrated flux of the n-KOM. The flux is again coded from black to red as it increases. It is plotted as a function of time (abscissa) and the system III longitude of Galileo (ordinates). Since the n-KOM is emitted radially [*Reiner et al.*, 1993], this plot gives the azimuthal position of the n-KOM sources in a reference frame that rotates with Jupiter. The lag of the sources with respect to the corotation is clearly apparent (progressive increase of their system III longitude). Using this plot, the creation of a new n-KOM source is easily detected as the sudden rise of strong radio flux at some precise system III longitudes.

In Plates 1g, 2g, and 3g, the maximum and the minimum of the local plasma frequency, measured for each rotation of Jupiter, are presented. Most of the time, when Galileo is far from Jupiter ($r > 25-30 R_j$), two density maxima per Jovian rotation are detected. This proves that Galileo entirely crosses the disc from one lobe to the other and thus measures the highest density corresponding to the central part of the disc. Nevertheless, the observation of two maxima per rotation is not systematic which indicate that the shape of the disc is sometimes strongly disturbed.

In Plates 1h, 2h, and 3h, the Galileo/Jupiter distance (thick line) and its longitude, calculated from the Jovian/Sun axis (Jovian/Sun coordinate system), are given.

The Galileo position during the G2, G7, and G8 PWS observations is presented with more detail in Figure 1. The interval between two symbols correspond to one Jovian rotation. The midnight/dawn sector of the magnetosphere was predominantly explored during the three orbits studied here, and one can consider that the observations have been performed in almost similar positions of Galileo in the magnetosphere but a few months apart. During the orbit G2,

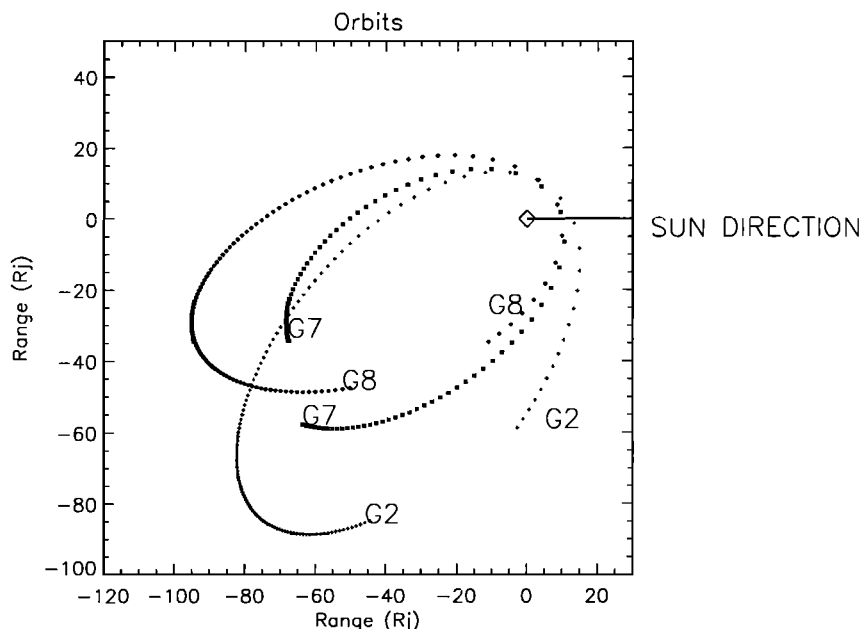


Figure 1. Galileo orbits in a Jovian/Sun coordinate system. The intervals between two symbols correspond to one planetary rotation.

PWS was active for a long period in the early morning side sector. This sector was also explored during G7 and G8 but for shorter periods and at closer distances from the planet (80 R_J instead of 120 R_J). During G7, PWS was also active during a long-lasting morningside exploration (from \sim 0300 MLT for $r=85 R_J$ to 0700 MLT for $r=22 R_J$). G8 is characterized by a complete radial cut of the magnetodisc around midnight.

Plates 1, 2, and 3 contain a considerable amount of information on the magnetodisc/plasma sheet structure as well as on the magnetospheric activity. They will be first studied in detail for identifying energetic events similar to those described in L98 and thus for surveying the bursty magnetospheric activity over a longer period of time than previously done.

3. Description of the Bursty Jovian Magnetospheric Activity

3.1. Identification of the Energetic Events

The identification criteria for the energetic events is the simultaneous observation of an increase in the flux of the auroral radio emissions and the creation of a new source of n-KOM. The occurrence of an event can be further confirmed by local plasma frequency measurements showing the existence of strong density fluctuations in the magnetodisc/plasma sheet. Together, these observations insure that a sudden energy release has taken place in the magnetosphere over a large spatial scale since it includes the Io torus, the auroral region and the distant magnetodisc. It is important to acknowledge that we have not developed a software able to automatically identify the events. A part of subjectivity thus remains in the procedure of visual inspection of the spectrograms and, as discussed later, some uncertainties could subsist in the identification (or non-identification) of a few events.

A good example of event is observed on DOY 96-272.5. At that time, the auroral radio flux roughly doubles for 10 to 20 hours and a new n-KOM source appears at around 320° of longitude. Sharp density fluctuations corresponding to crossings of extremely depleted plasma regions, as evidenced by the observation of a very low cutoff of the continuum radiation, are simultaneously detected. Furthermore, the event corresponds to an extension of the auroral radio emission towards lower frequencies (down to 200 KHz). This modification of the frequency bandwidth of the auroral emissions is observed for a majority of the events occurring during G2. Let us note that "simultaneous" must not be interpreted too rigorously here; rather, it means "within one planetary rotation". The emission cones of the different radio sources present important differences and a delay can then exist in the detection of flux variations that would simultaneously affect them. However, in any case, this delay cannot exceed 10 hours.

Using the above quoted identification criteria, 15 well-defined events are detected during G2, 9 during G7, and 10 during G8. They are indicated by vertical lines in Plates 1, 2, and 3 and listed in Table 1 where additional comments (relative amplitude of the auroral flux increases, simultaneous detection of short-scale fluctuations, presence of more progressive magnetodisc density evolutions) are made. These comments will be explained later in the text. We consider that there is no ambiguity for the events marked with an asterisk. For the period [97-086.5, 97-088.5], the situation is confused

since several events could have occurred with a particularly high frequency. We will, nevertheless, consider this period as one particular event. Additional perturbations could exist (for example, at DOY 97-140 and DOY 97-143.5). They have not been selected because the associated auroral flux enhancement is too modest (less than 10%) and/or they do not correspond to the creation of a clear new n-KOM source.

In conclusion, we identify without ambiguity 32 events during 130 days of observations distributed over a 245-day period. This corresponds to an average periodicity of 3.8 days, which is slightly longer than the 2.5 day periodicity previously reported from the examination of a restricted data set. The energetic events described in L98 from the analysis of a few days of observations are thus found to be regularly distributed over a much broader data basis. More generally, an examination of the complete set of PWS data shows that they are always present and thus actually representative of an important form of the Jovian magnetospheric dynamics.

3.2 – The Energetic Events as Signatures of Magnetospheric Energy Releases

We can use the data set in a different way. Let us consider that an increase of the auroral radio flux gives an indication for the existence of an enhanced dissipation in the auroral zones, then, for a particular energy release in the magnetosphere. It is then possible to select the periods of more powerful magnetospheric activity by examining Plates 1e, 2e, and 3e. Applying a simple criteria (selection of auroral radio flux variations larger than 10%), one can check that the association: (larger energy release/creation of new n-KOM sources) has a real statistical sense. With a high probability since only two significant auroral radio flux enhancements (at DOY 97-097 and 97-140) are not associated with a clear creation of a new n-KOM source, the phases of more intense magnetospheric activity (at least those associated with an enhanced auroral precipitation) are intimately associated with the occurrence of an energetic event. However, this does not mean that the energetic events always correspond to the strongest energy dissipation. For 8 out of 35 of the cases, the auroral radio flux continues to increase for a few Jovian rotations after the event (for example, DOY 96-263, 96-288, 97-105.5). As they are defined here (conjunction between auroral radio brightenings and creations of a new n-KOM sources), the energetic events indicate the beginning of periods lasting 20-40 hours of stronger energy dissipation in the magnetosphere. In that sense, they could be compared with the onset phase of terrestrial substorms.

Thus, if one admits that the auroral radio flux is a good proxy of the dissipation rate of the magnetospheric energy, then, in a rather systematic way, increases of this rate are associated with a largescale process affecting both the auroral region and the inner magnetosphere (Io torus). Moreover, it can be verified that in more than 60% of the cases (at least 23 over 35) the energy releases correspond to the observation of density perturbations in the plasma sheet which demonstrates their very global character. This not only confirms the results of L98 but also indicates that the beginning of periods of enhanced magnetospheric energy dissipation are almost systematically associated with an "energetic event".

3.3. Long-Term Variations of the Bursty Activity

Despite of the similarities in the characteristics of the individual events detected during G2, G7, and G8, the bursty

Table 1. Characteristics of the events

<i>Orbit G2</i>			
Date	Auroral Flux Increasing	Short Scale Plasma Fluctuations	Sudden Thickening and/or Progressive Thinning
96-253 *		not measurable	not measurable
96-255.8 *	+ 1.55	no	no
96-259.6 *	+ 2.29	no	yes
96-263 *	+ 2.14	yes	yes
96-264.4 *	+ 2.14	yes	yes
96-266.7 *	+ 1.55	yes	yes
96-270.2 *	+ 1.58	yes	no
96-272.6 *	+ 1.9	yes	no
96-275.1 *	+ 1.9	yes	yes
96-277.6 *	+ 1.58	yes	yes
96-280.3 *	+ 1.77	yes	yes
96-284.7 *	+ 1.41	yes	yes
96-288 *	+ 1.58	yes	yes
96-291.7 *	+ 1.25	yes	no
96-293.7 *	+ 1.6	no	not measurable
<i>Orbit G7</i>			
97-079.2 *	+ 1.6	yes	yes
97-083.3 *	+ 1.58	yes	yes
97-087.6	+ 1.35	not measurable	yes, difficult to measure
(disturbed period)			
97-091.7 *		not measurable	yes, difficult to measure
97-096 *		not measurable	not measurable
97-100.3 *	+ 1.69	yes	yes
97-102.3 *	+ 1.58	yes	yes
97-105.4 *	+ 1.41	yes	yes
97-109.3	+ 1.25	no	not measurable
<i>Orbit G8</i>			
97-133.3 *	+ 1.73	no	(*) progressive thinning long lasting period without event (~10 days)
97-142 *	+ 1.81	yes	reduced modulation
97-145 *			reduced modulation
97-149.1 *	marginal	yes	reduced modulation
97-152.5 *	+ 1.09	yes	progressive density increasing
97-154 *	> 2	yes	yes
97-158.2 *	+ 1.12	no	no
97-161 *	+ 1.58	yes	yes
97-164.4 *	+ 1.6	yes	yes
97-167.5 *	+ 1.8	yes	not measurable

activity also presents significant differences from one orbit to the other. One of them (see Plates 1b, 2b, 3b, 1e, 2e, and 3e) concerns the temporal evolution of the individual sources of n-KOM. For G2 the newborn sources are generally observed during three to four Jovian rotations and none of them lasts more than six rotations. The n-KOM thus vanishes between two successive creations of sources. Conversely, during G7 and G8 the n-KOM is almost continuously visible. From one source activation to the other and even for periods longer than 10 Jovian rotations, the n-KOM sources remain bright and their flux only slightly decays.

Other important differences concern the periodicity and the intensity of the energetic events. For G2 the average periodicity is 2.9 days (69.3 hours) compared to 4 days (95.1 hours) for G7. The situation for G8 is more complex. In the first part (before DOY 97-145) this orbit is characterized by an absence of events for a 10-day period. Later, a "normal" periodicity of 3.5 days is found again. The average auroral radio flux intensification is 1.73 for G2, 1.49 for G7, and 1.58 for G8. Some particularly intense events (increase by a factor larger than 2) are observed during G2; such intense events are not observed during G7 and G8.

In the terrestrial situation, the observation of a similar phenomena (variations in the periodicity and intensity of the substorms) would be related to a variability in the solar wind. The Jovian situation is likely quite different. We will try to relate the variations of the bursty activity to modifications of the internal characteristics of the magnetosphere. It has already been mentioned that the centrifugal stress could play an important role as a driver of the activity of the fast rotating Jovian magnetosphere. Among the different signs suggesting that this stress has varied in the inner magnetosphere, the observation of sudden density variations in the distant disc, interpreted in terms of global plasma motions from the internal magnetospheric regions, would be particularly interesting. We will then now more specifically analyze the evolution of the magnetodisc plasma density in association with the occurrence of the events.

4. Survey of the Magnetodisc/Plasma sheet Density

4.1. Long-Term Variations in the Magnetodisc Density

As seen in Plates 1g, 2g, and 3g the magnetodisc/plasma sheet is denser during G2 than during G7 and G8. During the 30 first days of the G2 orbit the maximum plasma frequency measured at each crossing of the central plasma sheet is well above 1 KHz. It typically ranges between 1.5 to 2.2 KHz, as Galileo was moving away from Jupiter from 30 R_j to more than 100 R_j . Later, it slightly decreases but still remains of the order of 800 Hz, except for a few day period around DOY 96-290. At comparable distances from Jupiter the maximum plasma frequency is smaller for both G7 and G8. At a distance of 60 R_j , it is around 2 KHz for G2, 1.5 KHz for G7 and 1 KHz for G8. Further away, at $r=80 R_j$ one gets 1.7 KHz for G2, 0.9 KHz for G7 and 0.7 KHz for G8. More precisely, while the maximum density has similar values at 30 R_j for the three orbits (0.05 cm^{-3} for both G2 and G7 and 0.04 cm^{-3} for G8), its radial variations beyond 30 R_j are different. The density remains almost constant over a large radial extent for G2 (a density of 0.03 cm^{-3} is still measured at 100 R_j) while it decreases to 0.008 cm^{-3} for G7 (at 80 R_j) and to less than 0.005 cm^{-3} for G8. The G7 and the G8 measurements described here have been performed in a similar local time sector (around 160°-180° of longitude in the Jovian/Sun coordinate system), a sector that has been also explored during G2 for $r < 70 R_j$. One can thus consider that the observed differences in the density cannot be due to spatial effects (possible variations in local time). They rather have to be attributed to temporal effects: the outer magnetodisc/plasma sheet was denser at the time of the G2 orbit than at the ones of G7 and of G8.

In an interesting way, the G2 orbit also corresponds to a more frequent occurrence of the events. This relationship between the periodicity of the events and the density in the magnetodisc seems to be relatively systematic. For example, the orbit G2 can be divided in two periods: (1) before DOY 96-280 the periodicity is 2.5 days and the average plasma frequency is of the order of 1.5 KHz; (2) later, the periodicity is 3.4 days and the plasma frequency has decreased to 800 Hz. For G8 the density continuously decreases for the long period without event (before DOY 97-142.6). The plasma frequency then progressively increases (from 800 Hz to more than 1.5 KHz), from DOY 97-140 to 97-158, as the periodicity of the events is again of the order of 3 days. In

both cases, Galileo has moved from the midnight to the morningside sector. The observed inverse evolution of the density (decrease for G2, increase for G8) thus cannot be simply related to local time variations (transition from midnight to the early morning sector).

Different scenarios may explain this global relationship between the frequency of the events and the magnetodisc density. A simple one would be that the events are associated with instabilities taking place in the distant disc (beyond 30-40 R_j). The observations reported here thus would indicate that the denser the disc is, the more unstable it becomes. Another explanation is possible: the events, linked to instabilities in the outer Io torus or in the close magnetodisc, would correspond to phases of enhanced radial plasma transport. The distant disc would thus be sporadically fed by new particle populations in relation with the events. Its density would be naturally larger as the frequency of events increases.

These two scenarios lead to an important observational difference. In the first case one expects to see the most heavily populated disc before the events. In the second case the plasma content would increase after the events. In order to identify a possible scenario, we will study the details of the modifications of the magnetodisc structure related to the occurrence of the events.

4.2. Phases of Apparent Thickening/Thinning of the Disc

A comparison of the maximum and minimum plasma frequency (Plates 1c, 2c, 3c and 1g, 2g, 3g) indicates that each event strongly affects the structure of the magnetodisc. It is important to notice that two different phenomena occurring over different timescales can be observed. First, in a majority of cases the events correspond to short-lasting (10-20 hours) sharp decreases of the minimum density (see DOY 96-266.7, DOY 96-270 for example) that are interpreted as the crossings of extremely depleted plasma regions (see the discussion in L98). Other interpretations are that the plasma sheet has thinned or that it has moved further from the spacecraft, leaving Galileo deeper in the lobe. Later, in a number of cases a much more progressive evolution of the density modulation is observed. It corresponds to a progressive divergence between the maximum and the minimum plasma frequency. This evolution is due to a decrease of the minimum density measured during the incursions into the lobes. The event 96-259.6 displays a good example of this evolution. During the period (96-259, 96-263), corresponding to eight planetary rotations, the maximum of the plasma frequency remains close to 1.5 KHz. Meanwhile, the minimum density continuously decreases from 800 to 200 Hz.

This effect is illustrated in a more systematic way in Figure 2 where both the maximum and the minimum densities measured for each crossing of the disc are plotted as a function of the time elapsed since the last event. These quantities are normalized to the values observed just after the sharp density fluctuations associated with the events. For example, in the case of the event 96-272.6 the sharp density fluctuations end at 96-273. We then choose quantities measured during the rotation (96-273.2, 96-273.6), when a well-defined disc is again observable, as references for the densities observed until 96-275, the date of the next event. Although the set of points present a considerable dispersion, a clear tendency appears: (1) the progressive decrease of the

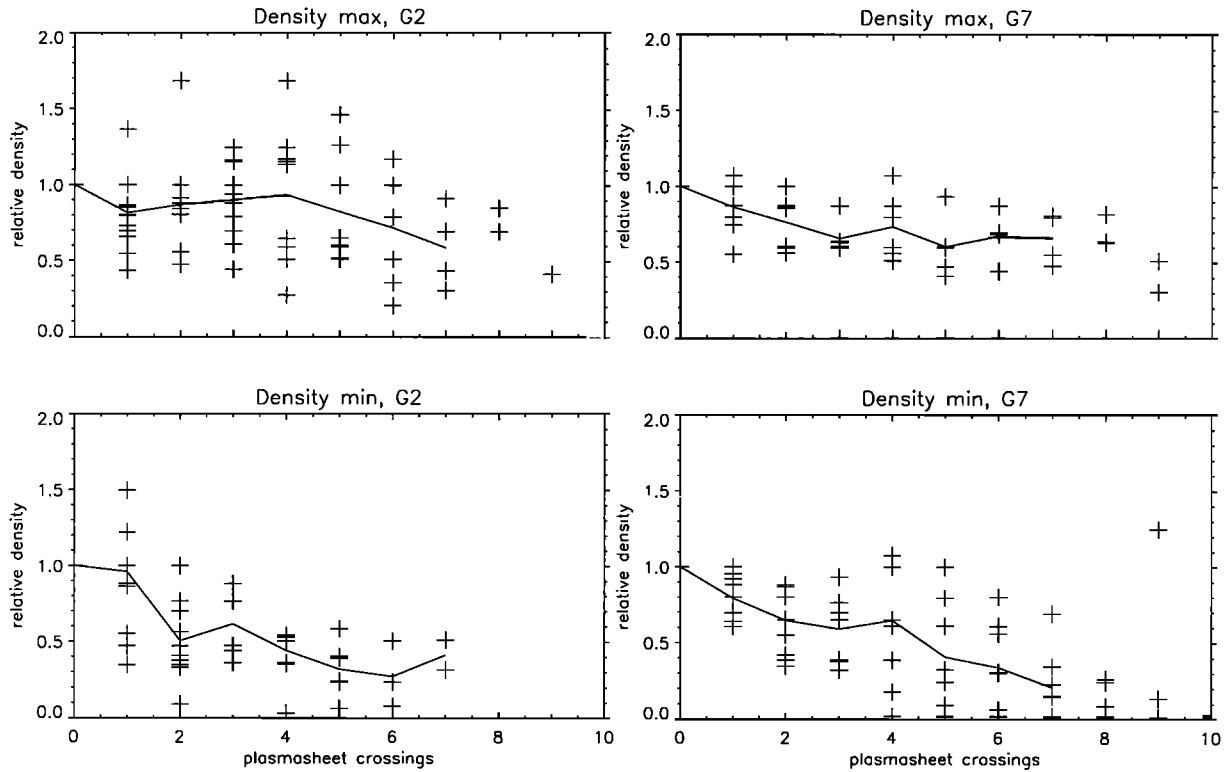


Figure 2. Evolution of the density in the magnetodisc as seen during successive disc crossings following the occurrence of the G2 and G7 events.

minimum density (decrease by a factor 3 to 4 in six to eight rotations), and (2) a less pronounced (20 to 30%) decrease of the maximum density over the same time period. This type of evolution is observed for a majority of events (9 over the 13 cases that can be studied for G2 and 7 over 7 for G7). The few exceptions indicate that other parameters could have an effect on the variations of the magnetodisc density. This study was not possible for G8 since the plasma density modulation is almost not visible from DOY 97-140 to DOY 97-109). 97-160. This corresponds to a time period during which Galileo is in the midnight meridian. During G7 the same type of low modulation of the density is observed for a similar position of Galileo in the magnetosphere (from DOY 97-105 to DOY 97-109). A possible interpretation would be that as suggested by Khurana [1992] the wobbling of the disc is reduced around midnight due to a "hinging" phenomena linked to the magnetosphere/solar wind interaction. This reduction of the wobbling precludes a study of the disc evolution.

The progressive evolution of the density reported here corresponds to an apparent thinning of the disc and to a decrease of its maximum density. It is observed after a majority of events for periods of a few tens of hours. It suggests that the magnetodisc plasma content is maximum just after the events and progressively decreases later on due to an evacuation of the plasma. The events thus do not preferentially occur as the plasma content of the disc is maximum but rather during the low-density situations resulting from the more or less long plasma evacuations. This observation favors our second hypothesis: the events correspond to periodic feedings of disc due to instabilities taking place close to the planet.

This important point must, however, be confirmed by a more careful examination since it suffers from ambiguities. If the variations of the maximum density are easy to follow, it is indeed more difficult to estimate the evolution of the plasma content of the magnetodisc. The amplitude of the disc wobbling has a strong influence on the observed density modulations and, in particular, the progressive increase of this modulation could well be explained by a modification in the wobbling instead of a disc thinning. In the next two sections, we will try to solve this ambiguity.

4.3. Models of the Density in the Central Sheet

In classical models of the plasma sheet density [Divine and Garrett, 1983], a simple exponential law describes the variation in the plasma density with respect to the distance from the central sheet:

$$n = N \exp \left[- \left(\frac{r\lambda - z_0}{H} \right)^2 \right] \quad (1)$$

where λ is the latitude, r the distance to Jupiter and z_0 the altitude of the central sheet above the equatorial plane. The shape of the central sheet is described by the variations of z_0 as a function of r , the longitude (l) and, possibly, the Jupiter-Sun-orbital plane (JSO) x coordinate (distance from Jupiter projected on the sun/planet axis). In a general way, one can write:

$$z_0 = A(r, x) \cos(l - \theta(r)) \quad (2)$$

where A is a function that describes the hinging of the central sheet and θ is an angle that varies with distance and describes

a warping of the disc due to a wave-like interaction between the inner magnetosphere and its external regions (for discussions on the shape of the disc, see *Kivelson et al.* [1978], *Goertz*, [1981], *Khurana and Kivelson* [1989], and *Khurana* [1997]). *Khurana* [1992] proposes the following expression for A :

$$A(r, x) = r \cdot \tan(9.6^\circ) \frac{x_0}{x} \tanh\left(\frac{x}{x_0}\right) \quad (3)$$

where $x_0 = 33.5 R_J$ as it is determined from a best fit with the observations of Voyager. This expression takes into account an effect of the solar wind that bends the disc towards the ecliptic plane in the noon/midnight sectors.

Using the above equations, a spacecraft close to the equatorial plane ($\lambda \approx 0$) would see a time varying local plasma density :

$$n(t) = N \exp\left[-\left(\frac{A \cos(\Omega t - \varphi)}{H}\right)^2\right] \quad (4)$$

From this equation it is a priori impossible to distinguish between a variation of the magnetodisc wobbling (temporal evolution of A) and a variation of its thickness (temporal evolution of H) by single spacecraft measurements of the density profile of the disc. A sudden reduction of the wobbling (owing to the fact that the magnetodisc is momentarily closer to the equatorial plane), followed by a progressive deformation that restore the classical hinged geometry, would explain the observations described above as well as a sequence of sudden thickening followed by a progressive thinning of the disc

Nevertheless, (4) corresponds to a very special type of density profile. The exponential profile is indeed defined by one parameter only (H) so that the variations of this single parameter describe the variations of the width of the plasma sheet. In such a case the simultaneous evolution of another parameter (A , corresponding to an evolution of the wobbling) would confuse the situation. The density profile can also be more complex so that two or more parameters are needed to describe it. A thinning of the disc or, more generally, a temporal evolution of the density profile could act differently on these parameters. Such an evolution would be impossible to model by the variation of a unique parameter thus by a simple evolution of the disc wobbling. As discussed in the next section this could solve the ambiguity.

4.4. Temporal Evolution of the Density in the Central Sheet

In order to better understand the dynamics of the disc a period of 96 hours of data, starting DOY 97-083, 0000:00, and corresponding to the event 97-083.5 has been specifically studied (Figure 3).

In Figure 3a, the integrated auroral radio flux (from 0.7 to 5.6 MHz, presented in unit of Vm^{-1}) is plotted. It presents the usual 10-hour modulation. The maximum flux is observed DOY 97-083 around 0800 UT. It can be verified that 10 hours before, during the preceding period of maximum visibility of the radio emissions, the flux is significantly smaller. Taking into account the 10-hour uncertainty, we thus estimate that the event occurs DOY 97-083 at 0300 ± 5 hours

UT, as indicated in Figure 3. In Figure 3b, the low-frequency part of the dynamic spectrum is displayed using a linear frequency scale. A black to white color code has been used. The continuum emission is in light gray and its low frequency cutoff is apparent as a sharp transition to black. The "arches" corresponding to the successive crossings of the central plasma sheet are referenced (0 to 14 as indicated above the plot). Below, in a series of eight plots, the density profiles corresponding to arches 0 to 7 are presented. In each case, 3 hours of data centered on the crossing of the central sheet are displayed. Finally, in Figure 3d, the maximum density observed during successive crossings of the central sheet is presented. Two methods have been used for determining these maxima: (1) direct measurements (crosses) and (2) selection after a sliding average (stars) in order to remove the possible effect of non significant short-lasting fluctuations. Figure 3 contains a wealth of information concerning the magnetodisc/plasma sheet dynamics associated with the occurrence of an event.

Let us first discuss timing. As indicated by the auroral radio flux, the event occurs before DOY 97-083, 0800 UT. Radiation at frequencies of the order of 100 KHz (not shown here) indicating the formation of the new n-KOM source are even detected before (DOY 97-083, 0400 UT). Owing to uncertainties in the exact timing, one can consider that the short-lasting density fluctuations (first seen DOY 97-083, 0600 UT), interpreted as the crossings of extremely depleted regions, are observed with a maximum delay of 2-4 hours with respect to the event. If it is interpreted in terms of a propagation from the inner magnetosphere, this delay corresponds to a propagation speed larger than 500 km/s, and thus in the Alfvénic range. As already noticed (see L98), these fluctuations could correspond to longitudinal disc disruptions that would thus propagate across the disc at a velocity of the order of the typical Alfvén velocity. It is only after this initial disturbed phase, with a typical delay of 10-20 hours, that the magnetodisc/plasma sheet recovers its normal structure as indicated by the reappearance of the regular 5-hour modulation.

Concerning the density evolution, for a period of almost 30 hours (from arch "1" to "6") following the reappearance of the normal magnetodisc, the density in the central sheet (see the plot of the maximum density) continuously decreases (from 0.05 to 0.02 cm^{-3}). The minimum density decreases even more sharply (from 0.015 to less than 0.001 cm^{-3}). As mentioned before, the evolution of the maximum density can be related to a plasma evacuation and the decrease of the minimum density to a thinning of the disc or to a stronger wobbling of the magnetodisc/plasma sheet. In view of an estimate of a possible variation of the mass of the disc, it is important to solve this ambiguity.

The study of the density profiles helps to better understand this evolution. Instead of being parabolic or exponential, the profile is rather trapezoidal, with plateau's at maximum. This is particularly clear for the arches 2, 4, 5, and 6. The density is almost constant (N_0) over a broad altitude range (H_0) above and below the center of the sheet. At larger distances from the central sheet it decreases over a variable length scale (ΔH) toward a constant value (N_f). This region of regular decrease of the density will be defined as the "flank" of the plasma sheet in the rest of the paper. A possible model for the density is then:

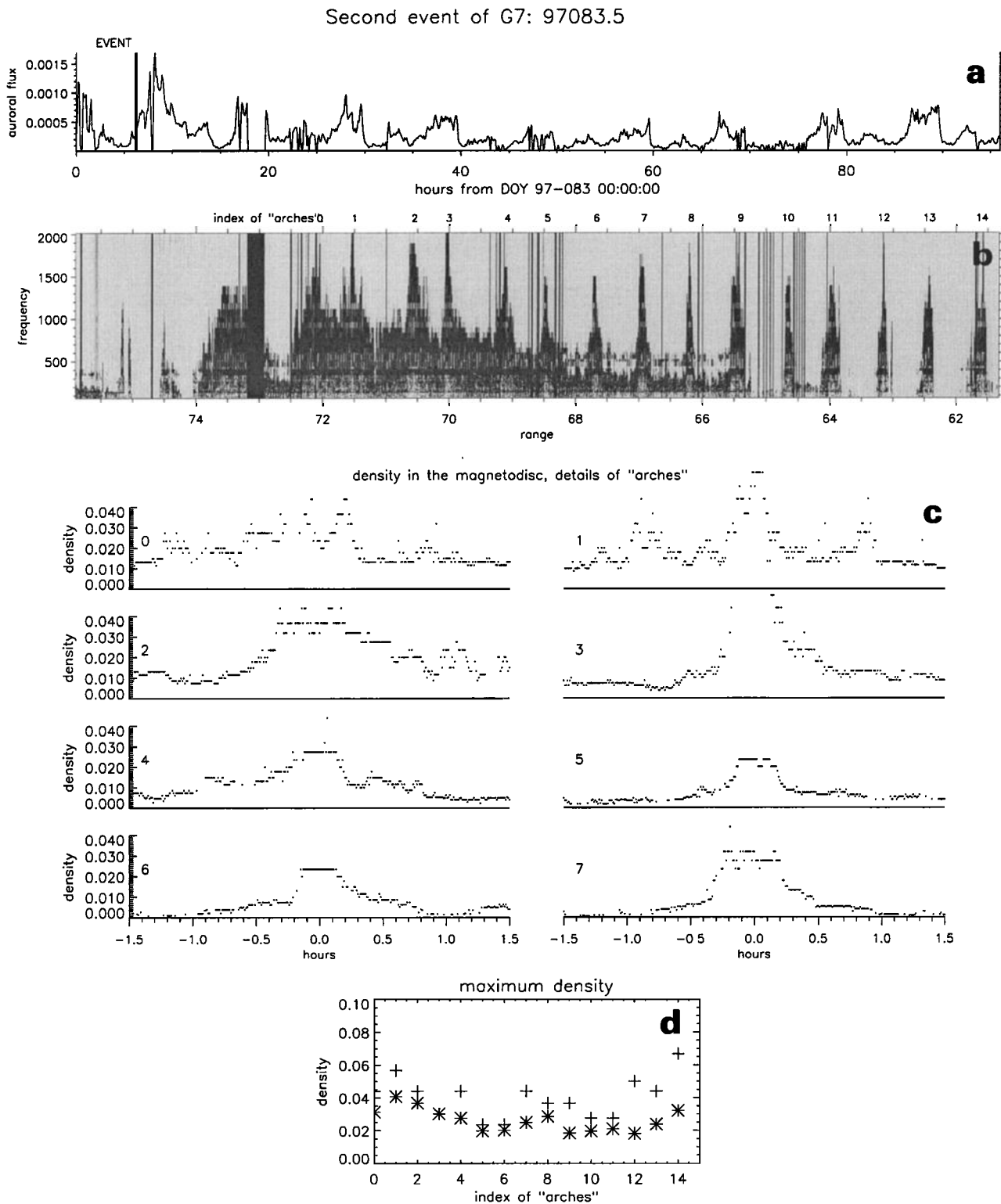


Figure 3. Spectrogram and density profiles observed after the event on DOY 97 083.5 (start time, DOY 97 083 0000:00). From top to bottom: (a) Average auroral flux. The event is expected to have occurred before the thick vertical line. (b) Spectrogram of the continuum radiation. The index of the "arches" are indicated at the top of the plot. (c) height density profiles (arches 0 to 7). (d) Evolution of the maximum density.

$$\begin{aligned}
 n &= N_0 \quad \text{for } |z - z_0| \leq H_0 \\
 n &= n(z) \quad \text{for } H_0 \leq |z - z_0| \leq H_0 + \Delta H \\
 n &= N_1 \quad \text{for } H_0 + \Delta H \leq |z - z_0|
 \end{aligned}
 \tag{5}$$

Let us note that Galileo does not reach altitudes larger than A above the central sheet (see (2)). The domain of observation is then restricted to $|z - z_0| < A$ and the density could decrease significantly below N_1 deeper in the lobes.

This type of density profile precisely corresponds to the complex situation (more than one parameter needed for its description) mentioned in section 4. Interestingly, with the exception of arches "0" and "2" the duration of the crossing of the plateau does not significantly vary. It remains of the order of 15 min. If δt is the crossing duration, using (3) and taking into account the planetary rotation, one obtains:

$$\delta t = \frac{1}{\Omega} \text{Arc sin} \left(\frac{2H_0}{A} \right) \approx \frac{1}{\Omega} \frac{2H_0}{A}
 \tag{6}$$

then, except if the variation of the thickness of the central sheet (effect related to a thinning) exactly compensates the variation of its height above the equatorial plane (effect related to a variation of the wobbling), one does not expect δt to be constant. The same reasoning applies to the parameter ΔH that is also rather constant from arches "3" to "7". This suggests that unless a very specific evolution corresponding to an exact compensation between the variation of the wobbling and the disc thinning has taken place, the shape of the disc does not significantly vary

Table 2. Observed characteristics of the plasma sheet

Arches	$N_0, \text{ cm}^{-3}$	$N_1, \text{ cm}^{-3}$	H_0, R_j	$\Delta H, R_j$
0	0.035 (?)	0.013 (?)	3.4 (?)	
1	0.05	0.013	0.9	0.9
2	0.04	0.012	2.6	2.6
3	>0.05	0.009	1.3	1.3
4	0.027	0.007	1.3	1.3
5	0.024	0.005	1.3	0.7
6	0.025	0.002	1.6	1.3
7	0.03	0.002	2	0.8

after the event. Both its width (H_0) and its wobbling have thus likely remained almost unchanged. The impression of an apparent thinning would be due to the progressive decrease of N_1 and more generally of the plasma density in the flanks of the sheet.

The evolution that follows the specific event described here is particularly clear so that the distinction between variation of the wobbling and thinning is relatively simple to make. It is, nevertheless, not a unique case. In Figure 4, we present another case (evolution after event DOY 96-259.6) for which we have plotted, as a function of the index of arch crossings after the events: (1) the duration of the crossing of the central sheet (defined as the region of density larger than 0.01 cm^{-3}) and (2) the minimum density observed during the incursions into the lobes. Except for two crossings (1 and 5), the crossing duration remains almost constant (around 65 min) during the period of 60 hours following the event analyzed here. Simultaneously, the minimum density in the lobe decreases by one order of magnitude. Again, such an evolution is consistent with an idea of a progressive plasma evacuation rather than a simple evolution of the wobbling. This can be used for quantifying the mass variation of the disc.

5. Quantitative Estimates of the Plasma Transport Associated to the Events

Assuming that the disc wobbling remains constant and using already published models of the current sheet, it is possible to estimate the variations of the plasma content of the disc associated with the observed density evolution. From formula (3), one gets $A \approx 8.5 R_j$ for the Galileo position at the time of occurrence of the event ($x \approx 50 R_j, r \approx 75 R_j$). The height above (or below) the central sheet is then easily deduced using the time elapsed since the last crossing of the central sheet (δt):

$$z = 8.5 R_j \sin(2\pi \delta t / 600) \sim 8.5 R_j \sin(0.01 \delta t)
 \tag{7}$$

where δt is given in minutes. This formula is used in Table 2 for deducing the values of the parameters describing the density profile. In Table 2, the question marks indicate measurements that are only approximate. As already mentioned, one can assume that the thickness of the central

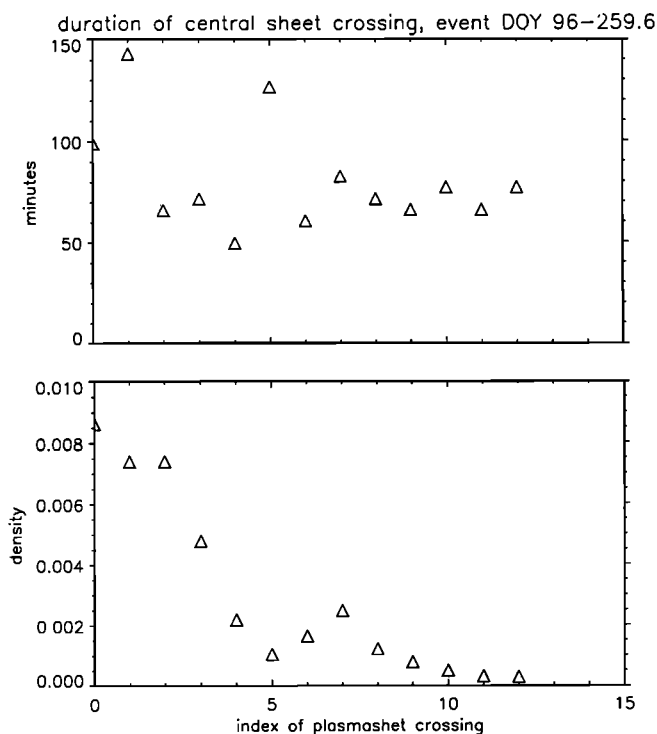


Figure 4. Second example of the evolution of the density profiles after an event (DOY 96 296.6): (top) duration of the current sheet crossing (bottom) minimum density seen in the lobes.

Table 3. Column density in the disc

Arches	Central Sheet 10^{13} m^{-2}	Flanks 10^{13} m^{-2}	Total 10^{13} m^{-2}
0	0.416	0.62	1.036
1	0.315	0.69	1.0
2	0.728	0.5	1.23
3	0.455	0.45	0.9
4	0.246	0.35	0.6
5	0.17	0.26	0.43
6	0.254	<0.1	0.354
7	0.304	<0.1	0.404

plasma sheet (H_0) does not significantly evolve. Its typical density, nevertheless, decreases by a factor 2 from arch 1 to 6 (see Figure 3d). More spectacular is the evacuation of the plasma from the flanks of the sheet over a scale height of the order of A ($8.5 R_J$). H_f indeed decreases by 1 order of magnitude (from 0.015 to less than $2 \cdot 10^{-3} \text{ cm}^{-3}$) from arch 1 to 6.

As illustrated by this particular example, the details of the plasma evacuation process would be the following:

After the initial phase of strong density fluctuations that immediately follows the event, a dense central magnetodisc/plasma sheet, with significantly populated flanks, is observed. Then, during a second phase, the density in the central region progressively decreases (variation of N_0) and the plasma in the flanks is evacuated (over a 40-hour timescale here). The parameters given in Table 2 can be used for estimating the typical column density in the disc (Table 3) and studying its temporal variations. We have here considered that due to multiple charged ions, the ion density is roughly half of the electron one (see the plasma composition of the outer magnetodisc given by *Divine and Garrett*, [1983]). The column density in the central sheet is given by the formula: $N_0 (H_0 + \Delta H)$, and, in the flanks by: $N_f (17 R_J - (H_0 + \Delta H))$. We here assume that the density N_f is observed over a scale height of $2 A$ (then $17 R_J$) which actually corresponds to the maximum incursion of Galileo toward the lobes. As seen in Table 3, the total column density decreases by a factor of the order of 3 in 30-40 hours. Next, in order to obtain an order of magnitude of the total quantity of matter involved in the phenomena, the surface of the disc concerned by the density variations must be estimated. Two points are worth noting. First, the plasma evacuation from the disc is systematically observed for successive crossings of the plasma sheet (then for lobe-to-lobe cuts performed at 180° of longitude one to the other). The density variations (at least when it is seen in the distant disc) thus certainly take place over the complete angular range (2π). Second, concerning their possible radial extension, the thinning phenomena are observed for positions of Galileo ranging from typically 40 to $120 R_J$. Given this broad radial range of the observations and the fact that the plasma evacuations are low-evolution processes observed over a few tens of hours timescale, it seems difficult to interpret them as short radial scale deformations of the disc that would be slowly convected outward. A global evolution of the magnetodisc is thus certainly more plausible. Taking into account these numbers, one comes to the conclusion that the total disc surface where

the density variations take place is of the order of $2 \times 10^{20} \text{ m}^2$ (corresponding to $\pi (120^2 - 40^2) R_J^2$). Using this value, the following global quantities of matter are obtained: (1) for the central sheet: 2.5×10^{33} ions (arch 2) at maximum and 0.6×10^{33} ions (arch 5) at minimum, and for the flanks: 2.5×10^{33} ions (arch 1) at maximum and less than 0.36×10^{33} ions (arch 6) at minimum. In the present case this evolution takes place in 20-25 hours (around $8 \cdot 10^4 \text{ s}$). A total flux of the order of 5×10^{28} ions/s is thus obtained for the overall process. This is larger than the ion production rate at Io observed directly from Galileo during the Io fly by in 1995 [*Bagenal*, 1997].

The example discussed here displays a particularly pronounced evolution and the estimated mass variation can be considered as a maximum value. The averaged evolutions of the minimum and maximum densities shown in Figure 2 suggest that the magnetodisc plasma content would typically decrease by a factor of 2 over 30-40 hours. Starting with 3×10^{33} ions in the plasma sheet, one gets an evacuation rate of the order of 1.4×10^{28} ions/s, which still corresponds to an important part of the expected plasma production rate of Io.

Obviously, there are a number of uncertainties in these estimates. The most difficult quantity to estimate is the amplitude of the wobbling (value of $A(r,x)$) from which the width of the plasma sheet is deduced. The value chosen here ($8.5 R_J$), from Khurana's model, is certainly not unreasonable and similar values would be found using other published models. The central point of our demonstration is rather the assumption of a relatively unchanged shape of the central sheet (constant wobbling) during the density evolution. To invalidate our conclusion (the observed plasma evacuation rate is a significant fraction of the Io production rate), the quantity of matter calculated for arch "2" would have to be reduced by a factor 3. This could be accounted for by a similar reduction of A . However, this would mean that the events correspond to very strong deformations of the shape of the central sheet, a point particularly difficult to reconcile with the observations of a relatively constant width of the central sheet (section 4.3). Unless large and specific deformations of the disc systematically occur after the events (compensation of the effects of the disc thickening and the wobbling evolution), our conclusion remains valid: the events correspond to significant radial plasma transport across the magnetosphere, with total magnitude of the order of Io's production rate.

6. Discussion and Conclusion

Studying PWS data registered during orbits G2, G7, and G8, we get the following observational facts :

1. Energetic events identified from the simultaneous observations of enhanced auroral radio emissions, creation of new n-KOM sources and perturbations of the plasma density in the magnetodisc/plasma sheet are recurrently detected by the PWS experiment (section 3.1). Their frequency varies from 2.5 days (orbit G2) to more than 4 days (orbit G7) with one example of a particularly quiet period (no event for 10 days during orbit G8).

2. The auroral radio flux typically doubles during the events. They are thus likely to be associated with strong increases of the auroral activity (section 3.2). More precisely, the events correspond to the beginning of periods lasting 10

to 40 hours of enhanced auroral activity. An analogy with the Earth magnetospheric activity thus suggests that the events mark the onset of periods of stronger energy dissipation in the magnetosphere. Reciprocally, the examination of these 130 days of observations distributed over a period of 9 months shows that the periods of enhanced dissipation are almost systematically initiated by energetic events.

3. The typical magnetodisc/plasma sheet plasma density seems to increase as the events become more frequent (sections 3.3 and 4.1). The density is thus typically twice as large for G2 (2.9-day periodicity) than for G7 and G8 (4-day periodicity).

4. The study of the magnetodisc/plasma sheet density perturbations associated with individual events helps to understand this relationship (sections 4.2, 4.3, and 4.4). Each event indeed corresponds to a phase of enhanced radial plasma transport. Just after the events a dense and thick magnetodisc is rather systematically observed (Figure 2). Then, over a few tens of hours timescale both the densities in the central sheet and in the flanks of the plasma sheet decrease. This leads to an apparent thinning of the disc which likely correspond to a progressive evacuation of the plasma.

5. A related important point is that before the occurrence of an event, one does not see a progressive increase of the density in the magnetodisc. It would indeed be possible to imagine that the phases of enhanced plasma evacuations would be the result of instabilities taking place in the distant disc after a more or less long progressive plasma loading of the whole magnetodisc. Clearly, it is not the case: the events suddenly occur as Galileo, in the distant disc, sees a low populated plasma sheet. It is only after the periods of observation of sharp density fluctuations (interpreted as longitudinal disc disruptions in L98), lasting 10 to 30 hours at maximum, that a dense disc is observed.

6. Assuming that the local density perturbations seen during and after the events have a broad angular and radial extension, which is supported by the fact that they are almost systematically observed after each event, in the whole magnetospheric region explored by Galileo, the phases of sudden density increases and progressive decreases correspond to a global plasma evacuation rate comparable to the Io production rate (section 5).

These observations lead to some important conclusions concerning the activity of the Jovian magnetosphere and its mechanism of internal radial plasma transport. They are indeed consistent with a scenario of the radial plasma transport in which the energetic events correspond to instabilities taking place in the external regions of the Io torus or in the close magnetodisc (10 to 20 R_J) and leading to sporadic injections of plasma in the distant magnetodisc/plasma sheet. This ejected plasma has an initial radial velocity that would be likely a non-negligible fraction of its initial rotational velocity (of the order of 200 km/s). This radial velocity is thus sufficient for the ejected plasma to reach distant regions of the disc during the phases of the strong density fluctuations that immediately follow the events and that last 10-20 hours. As a result of this plasma loading, at some distances from Jupiter and after the perturbed period a thick and dense disc is suddenly observed. Then, a plasma evacuation process leads to a progressive decrease of the plasma density inside the central sheet and in its flanks. The global plasma content of the plasma sheet would thus

present "sawtooth" variations, and, not surprisingly, it increases in average as the frequency of the events increases. This transport mechanism would be efficient enough for explaining the radial transport of an important part of the plasma produced by Io, which constitutes one of the major conclusions of the present work.

The present interpretation of the PWS observations could have some consequences for the classical conceptions of the radial plasma transport in fast rotating magnetospheres. If relatively small scale transport processes (including the interchange of flux tube of limited extension, see Kivelson *et al.* [1997]) could play a role in the Io torus, the outward radial transport from this plasma reservoir seems to be dominated by large scale explosive processes (along this line, see Yang *et al.* [1994]). The precise nature of this ejection mechanism remains unknown. However, the observations reported here suggests that the centrifugal stress in the external Io torus/close magnetodisc is important as a driver of the bursty Jovian activity. Consequently, the Io plasma production rate and possibly, variation of this rate, would be an important controlling factor of the magnetospheric dynamics and of its characteristics. This point must nevertheless be confirmed by future studies.

Acknowledgments. The French part of this work has been supported by CNES and CNRS.

Michel Blanc thanks Michael Kaiser and Fritz M. Neubauer for their assistance in evaluating this paper.

References

- Bagenal, F., The ionization source near Io from Galileo wake data, *Geophys. Res. Lett.*, **17**, 2111, 1997.
- Barrow, C. H., and M. D. Desch, Solar wind control of Jupiter's hectometric radio emission, *Astron. Astrophys.*, **213**, 495, 1989.
- Desch, M. D., and C. H. Barrow, Direct evidence for solar wind control of Jupiter's hectometer-wavelength radio emission, *J. Geophys. Res.*, **89**, 6819, 1984.
- Dessler, A. J., Preface, *Physics of the Jovian Magnetosphere*, edited A. J. Dessler, pp. XIII – XV, Cambridge Univ. Press, New York, 1983.
- Divine, N., and H. B. Garrett, Charged particles distributions in Jupiter's magnetosphere, *J. Geophys. Res.*, **88**, 6889, 1983.
- Fazakerley A. N., and D. J. Southwood, Drift waves, magnetospheric interchange instability and plasma transport in the magnetosphere of Jupiter, *J. Geophys. Res.*, **97**, 10,787, 1992
- Ferrière K. M., and M. Blanc, Plasma transport in rapidly rotating magnetospheres: general equations, *J. Geophys. Res.*, **101**, 19,871, 1996.
- Ferrière K. M., C. Zimmer, and M. Blanc, Magnetohydrodynamic waves and gravitational/centrifugal instability in rotating systems, *J. Geophys. Res.*, **104**, 17,335, 1999.
- Gérard, J.C., V. Dols, F. Paresce, and R. Prangé, Morphology and temporal variations of the UV aurorae of Jupiter with HST, *J. Geophys. Res.*, **98**, 18,793, 1993.
- Goertz, C.K., The orientation and motion of the predawn current sheet and Jupiter's magnetotail, *J. Geophys. Res.*, **86**, 8429, 1981.
- Goldreich, P., and D. Lynden-Bell, Io: A Jovian unipolar inductor, *Astrophys. J.*, **159**, 59-78, 1969.
- Gurnett, D.A., W.S. Kurth, and F.L. Scarf, The structure of the Jovian magnetotail from plasma wave observations, *Geophys. Res. Lett.*, **7**, 553, 1980.
- Gurnett, D. A., W. S. Kurth, R.R. Shaw, A. Roux, R. Gendrin, C. F. Kennel, F. L. Scarf, and S. D. Shawhan, The Galileo plasma waves investigation, *Space Sci. Rev.*, **60**, 341, 1992.
- Hill, T. W., Interchange stability of a rapidly rotating magnetosphere, *Planet. Space Sci.*, **24**, 1151, 1976.
- Hill, T. W., Inertial limit on corotation, *J. Geophys. Res.*, **84**, 6554, 1979.

- Hill, T. W., and A. J. Dessler, Plasma motion in planetary magnetosphere, *Science*, 252, 410, 1991.
- Hill, T. W., A. J. Dessler, and C. K. Goertz, Magnetospheric models, in *Physics of the Jovian Magnetosphere*, edited by A. J. Dessler, p. 353, Cambridge Univ. Press, New York, 1983.
- Jones, D., Io plasma torus and the source of Jovian narrow-band kilometric radiation, *Nature*, 327, 492-495, 1987.
- Kaiser, M. L., Time-variable magnetospheric radio emissions from Jupiter, *J. Geophys. Res.*, 98, 18757, 1993.
- Kaiser, M. L., and M. D. Desch, Narrow-band Jovian kilometric radiation: a new radio component, *Geophys. Res. Lett.*, 7, 389, 1980.
- Kennel, C. F., and F. Coroniti, Is Jupiter's magnetosphere like a pulsar's or Earth's, In *Magnetosphere of the Earth and Jupiter*, edited by V. Formisano, 451, D. Reidel, Norwell Mass., 1975.
- Kivelson, M. G., P. J. Coleman, L. Froidevaux, and R. L. Rosenberg, A time dependent model of the Jovian current sheet, *J. Geophys. Res.*, 83, 4823, 1978.
- Kivelson, M. G., K. K. Khurana, C. T. Russell, and R. J. Walker, Intermittent short-duration magnetic field anomalies in the Io torus: Evidence for plasma interchange?, *Geophys. Res. Lett.*, 24, 2127, 1997.
- Khurana, K. K., A generalized hinged-magnetodisc model of Jupiter's nightside current sheet, *J. Geophys. Res.*, 97, 6269, 1992.
- Khurana, K. K., Euler potential models of Jupiter's magnetospheric field, *J. Geophys. Res.*, 102, 11295, 1997.
- Khurana, K. K., and M. G. Kivelson, On Jovian plasma sheet structure, *J. Geophys. Res.*, 94, 11791, 1989.
- Krupp, N., J. Woch, A. Lagg, B. Wilken, S. Livi, and D. J. Williams, Energetic particle bursts in the predawn Jovian magnetotail, *Geophys. Res. Lett.*, 24, 1249, 1998.
- Kurth, W.S., and D.A. Gurnett, Auroral kilometric radiation integrated power flux as a proxy for Ae, *Adv. Space Res.*, 22, 73, 1998.
- Kurth, W.S., D. D. Barbosa, F. L. Scarf, D. A. Gurnett and R. L. Poynter, Low frequency radio emissions from Jupiter: Jovian kilometric radiation, *Geophys. Res. Lett.*, 6, 747, 1979.
- Kurth, W. S., D. A. Gurnett, S. J. Bolton, A. Roux, and S. M. Levin, Jovian radio emissions, an early overview of Galileo observations, in *Planetary Radio Emissions IV*, edited by H.O. Rucker and A. Lecacheux, Austrian Acad. of Sci. Press, Vienna, 1998.
- Ladreiter, H. P., P. Zarka, and A. Lecacheux, Direction-finding study of the Jovian hectometric and broadband kilometric radio emissions: Evidence for their auroral origin, *Planet. Space Sci.*, 42, 919, 1994.
- Leblanc, Y., The kilometric Jovian radio sources at the Io torus, in *Planetary Radio Emissions III*, edited by H. O. Rucker, S. J. Bauer, and B. M. Perdersen, p. 149, Austrian Acad. of Sci., Graz, 1987.
- Louarn, P., A. Roux, S. Perraut, W.S. Kurth, and D.A. Gurnett, A study of the large scale dynamics of the Jovian magnetosphere using the Galileo plasma wave experiment, *Geophys. Res. Lett.*, 25, 2905, 1998.
- Perraut, S., A. Roux, P. Louarn, D.A. Gurnett, W.S. Kurth, and K.K. Khurana, Mode conversion at the Jovian plasma sheet boundary, *J. Geophys. Res.*, 103, 14,995, 1998.
- Pontius D. H., and T. W. Hill, Rotation driven plasma transport: The coupling of macroscopic motion and microdiffusion, *J. Geophys. Res.*, 94, 15,041, 1989.
- Prangé, R., D. Rego, D. Southwood, P. Zarka, S. Miller, and W. Ip, Rapid energy dissipation and variability of the Io Jupiter electrodynamic circuit, *Nature*, 379, 323, 1996.
- Reiner, M. J., J. Fainberg, R. G. Stone, M.L. Kaiser, M. D. Desch, R. Manning, P. Zarka, and B.M. Perdersen, Source characteristics of the Jovian narrow-band kilometric radio emissions, *J. Geophys. Res.*, 98, 13,163, 1993.
- Southwood, D. J., and Kivelson M. G., Magnetospheric interchange instability, *J. Geophys. Res.*, 92, 109, 1987.
- Vasyliunas, V. M., Plasma distribution and flow, in *Physics of the Jovian Magnetosphere*, edited by A. J. Dessler, p. 395, Cambridge Univ. Press, New York, 1983.
- Woch, J., N. Krupp, J. A. Lagg, B. Wilken, S. Livi, D. J. Williams, Quasi-periodic modulations of the Jovian magnetotail, *Geophys. Res. Lett.*, 24, 1253, 1998.
- Yang, Y. S., R. A. Wolf, R. W. Spiro, T. W. Hill, and A. J. Dessler, Numerical simulation of torus-driven plasma transport in the Jovian magnetosphere, *J. Geophys. Res.*, 99, 8755, 1994.
- Zarka, P., Auroral radio emissions at the outer planets: Observations and theories, *J. Geophys. Res.*, 103, 20,159, 1998.
- Zarka, P., and F. Genova, Low frequency Jovian emission and the solar wind magnetic sector structure, *Nature*, 306, 767, 1983.

D. Gurnett and W. Kurth, Department of Physics and Astronomy, University of Iowa, Iowa City, IA 52242.

P. Louarn, Centre d'Etudes Spatiales des Rayonnements, 9, Avenue du Colonel Roche, B. P. 4346. 31028, Toulouse Cedex 4, France. (philippe.louarn@cesr.fr)

S. Perraut and A. Roux, Centre d'Etudes des Environnements Terrestre et Planétaires, 10-12, Avenue de l'Europe, 78140, Velizy, France.

(Received May 25, 1999; revised September 8, 1999; accepted October 1, 1999.)